

EXPERIMENTAL ASPECTS OF HYPERNUCLEAR PHYSICS AT CEBAF

Bernhard A. Mecking
CEBAF
12070 Jefferson Avenue
Newport News, Virginia 23606

ABSTRACT

The general features of the electromagnetic excitation of hypernuclei are outlined. Experimental aspects of investigating these reactions at CEBAF are discussed. Two specific experimental set-ups are compared.

- A. Introduction
- B. Features of the Electromagnetic Excitation of Hypernuclei
- C. General Experimental Considerations
- D. Two Experimental Set-ups for CEBAF
- E. Summary and Conclusions
- F. References

A. Introduction

One of the exciting aspects of a high duty-cycle, multi-GeV electron accelerator is the possibility to study the excitation and the decay of hypernuclei (nuclei in which one nucleon is replaced by a hyperon, usually a Λ). In the multi-nucleon system, the hyperon can be viewed as a controlled impurity which lives long enough to sample its hadronic environment and also is not restricted by the Pauli principle (except maybe at the quark level). Most of our present knowledge on the level scheme of nuclei comes from (K^-, π^-) exchange reactions /1/. The (K^-, π^-) reaction offers the big advantage that, at the right K^- momentum, the mass difference between a Λ and a nucleon can be compensated by the $K-\pi$ mass difference. This leads to recoilless Λ -production with correspondingly high cross sections for the formation of hypernuclei. Only modest overall energy resolution has been reached (2-3 MeV), mainly limited by energy loss in the target /2/). The big disadvantage of the (K^-, π^-) reaction is, however, the large distortion introduced by both the incident K^- and the outgoing π^- making the study of heavy hypernuclei impossible and, generally, a quantitative interpretation of the results difficult.

In contrast to the (K^-, π^-) reaction, the electromagnetic excitation of hypernuclei (using the $\gamma p \rightarrow K^+ \Lambda$ process to transform a proton into a Λ) offers the advantage that the nucleus is practically transparent to the incident probe. In addition, K^+ have less interaction than K^- (the \bar{u} -quark in the K^- can easily annihilate with a valence quark in the nucleon to form a 3-quark resonance, the \bar{s} quark in the K^+ can only annihilate with a sea quark). The combination of the clean production mechanism and the low distortion make the electromagnetic excitation of hypernuclei an excellent program for a multi-GeV electron accelerator. There are, however, serious experimental problems that have to be solved first: to get sufficient count rate and resolution for the excitation energy of the final hypernucleus.

B. Features of the Electromagnetic Excitation of Hypernuclei

The cross section for the electromagnetic excitation of hypernuclear levels are mainly governed by

- a) the cross section for the elementary $\gamma p + K^+ \Lambda$ reaction
- b) the transition form factor (nucleus + hypernucleus) which depends critically on the momentum transfer to the hypernucleus q and on the characteristics of the hypernuclear level.

The cross section for the elementary $\gamma p + K^+ \Lambda$ reaction is not well known and should be the subject of an independent experimental study. Examples for the existing data are presented in fig. 1 /3/. For the $A=12$ system, the momentum transfer q for $\gamma A + K^+ \Lambda_A$ is shown in fig. 2 as a function of the K^+ laboratory angle and the primary photon energy E_γ . Reasonably small momentum transfers are reached for high photon energy ($E_\gamma \geq 1.5$ GeV) and small kaon angles ($\theta_K \leq 10^\circ$). With increasing photon energy, the momentum transfer for 0° kaons decreases. The angular range, however, in which small momentum transfer can be reached, shrinks with increasing photon energy. For counting rate estimates, it is therefore necessary to average the cross section over the aperture of the experimental apparatus.

The differential cross section for the excitation of hypernuclear levels has been calculated by several authors /3-8/. For the following counting rate examples, the calculation by T.W. Donnelly /3/ for the transition $\gamma \text{ }^{12}\text{C} + K^+ \text{ }^{12}\text{B}_\Lambda(1^- \text{ g.s.})$ has been adopted. At $E_\gamma = 2$ GeV ($E_0 = 4$ GeV, $E' = 2$ GeV)

$$d^3\sigma/d\Omega_K d\Omega_e dE_e = 7 \cdot 10^{-35} \text{ cm}^2/\text{sr}^2 \cdot \text{GeV} \quad \text{for } (e, e' K^+)$$

$\theta_e = 15^\circ$ and $\theta_K = 15^\circ$ (kaon emitted in the direction of the virtual photon). Larger cross sections can be obtained by detecting both e^-

and K^+ at smaller angles. For a high luminosity set-up, this will lead to considerable experimental difficulties because of the high background rates. For real photons with $E_\gamma = 2$ GeV, Donnelly obtains

$$d\sigma/d\Omega_{\mathbf{K}} = 1.1 \cdot 10^{-31} \text{ cm}^2/\text{sr} \text{ at } \theta_{\mathbf{K}}=0^\circ \text{ for } (\gamma, K^+)$$

Note that these cross sections have been calculated in the framework of a non-relativistic model. Relativistic calculations are still in their infancy. First attempts to calculate hypernuclear excitation fully relativistically lead to smaller cross sections /7,8/.

To optimize the design of experimental equipment, it is useful to parametrize the cross section in terms of the photon energy and the transferred momentum $q(E_\gamma, \theta_{\mathbf{K}})$, e.g.

$$d\sigma/d\Omega_{\mathbf{K}} = G(E_\gamma) \cdot \exp(-(q/p_0)^2)$$

where $G(E_\gamma)$ describes the photon energy dependence of the elementary production process, and the exponential takes care of the nuclear transition form factor (p_0 was adjusted to reproduce the theoretical calculation /3/). This parametrization allows to predict the cross sections at arbitrary photon energies and kaon angles; examples are given in fig. 3. The integration over the experimental kaon acceptance can now be performed. The averaged cross section, shown in fig. 4, exhibits a broad maximum around $E_\gamma \approx 2.2$ GeV; reasonable values are obtained above 1.5 GeV. (The details depend, of course, on the specific nuclear level involved.)

C. General Experimental Considerations

For the first round of experiments, the highest priority is to demonstrate that the electromagnetic production of hypernuclei can be observed with sufficient energy resolution and reasonable counting rates.

In the initial stage, there is no urgent need to vary Q^2 (4-momentum squared of the virtual photon). Note that, for virtual photons, the minimum momentum transfer to the hypernucleus is always higher than for real photons.

In addition to the level scheme, the transition form factor has to be determined for each level. Experimentally, the easiest way to change the momentum transfer to the hypernucleus (not to be confused with the Q of the virtual photon) is to change the angle of the outgoing K^+ relative to the direction of the real or virtual photon.

The electromagnetic production of hypernuclei will be especially useful if high resolution for the excitation energy of the hypernucleus can be reached. While ≈ 1 MeV resolution will allow to investigate selected levels in light nuclei, a whole new field (especially for heavy hypernuclei) would be opened up by ≈ 100 keV resolution (see T.W. Donnelly's ratings /9/).

A reasonable photon energy range is around 1.5 GeV. Although the forward cross section goes up with increasing photon energy, it becomes more and more difficult to achieve the high absolute resolution required and to cover a large solid angle. The optimum operating point will depend on the maximum momenta, the solid angles and the resolution of the magnetic spectrometers available (and, of course, on the nuclear level involved).

The K^+ counting rate is reduced by kaon decay in the spectrometer. The kaon survival probability ϵ_K is

$$\epsilon_K = \exp(-L/\beta_K \cdot \gamma_K \cdot L_0)$$

where L is the total length of the spectrometer, L_0 is the decay length of the kaon: $L_0 = 371$ cm and $\gamma_K = E_K/m_K$. In practice, going to higher incident energies, and therefore to higher kaon momenta, does not increase ϵ_K because the total length L of high resolution ($\leq 10^{-4}$)

spectrometers scales roughly linearly with the maximum momentum: $L=C \cdot p$ with $C \approx 10$ meter/GeV/c. Therefore, the survival probability ϵ_K becomes a constant independent of the choice of the photon energy:

$$\epsilon_K = \exp(-C \cdot p_K \cdot m_K / \beta_K \cdot E_K \cdot L_0) = \exp(-C \cdot m_K / L_0) \approx 0.25$$

In general, the coincidence cross section peaks for K^+ being emitted in the direction of the real or virtual photon. In that direction there will also be a high rate of coincident positrons from e^+e^- pair production. A possible way to get rid of the e^+ (especially important for the trigger) is to block the central part of the kaon spectrometer acceptance mechanically. Remaining e^+ will have to be separated from K^+ by using a combination of Cerenkov and shower counters. Note that, ideally, K^+ identification is accomplished by the focal plane detector in the kaon spectrometer without using the time-of-flight between the target and the focal plane. Using the time-of-flight measurement to clean up insufficient particle identification will increase the random noise (e.g. due to accidental pion-electron coincidences). Also, the kaon momentum resolution will be spoiled due to the detection of coincident particles from the kaon decay.

D. Two Experimental Set-ups for CEBAF

Real and accidental rates as well as the expected missing mass resolution will be compared for two different experimental arrangements:

1. $(e, e'K^+)$ with finite θ_e and θ_K (around 15°)
2. $(e, e'K^+)$ with $\theta_e \approx 0^\circ$

1. $(e, e'K^+)$, θ_e and θ_K around 15°

The present design of the CEBAF high resolution spectrometers /14/ aims at a minimum separation of about 30° between the electron and the hadron spectrometer. Due to the low flux of virtual photons at large electron scattering angles, this set-up requires a high current of incident electrons and well shielded detector systems.

a) True coincidence rate for θ_e and θ_K around 15°

The true coincidence rate N_{eK} is calculated under the assumptions

incident flux	$N_e = 6 \cdot 10^{14} / \text{sec}$ (I=100 μ A)
target thickness	$\rho \cdot d = 100 \text{ mg/cm}^2$ (^{12}C)
luminosity	$L = 3.6 \cdot 10^{37} \text{ cm}^{-2} \cdot \text{sec}^{-1} / \text{nucleon}$
initial e^- energy	$E_e = 4 \text{ GeV}$
final e^- energy	$E_e = 2 \text{ GeV}$
e^- solid angle	$\Delta\Omega_e = 10 \text{ msr}$
e^- momentum acceptance	$\Delta E_e / E_e = 10 \%$
K^+ solid angle	$\Delta\Omega_K = 10 \text{ msr}$

$$\begin{aligned}
 N_{eK} &= L/A \rho d \frac{d^3\sigma}{d\Omega_K d\Omega_e dE_e} \cdot \Delta\Omega_e \cdot \Delta\Omega_K \cdot \Delta E_e \cdot N_e \cdot \epsilon_K \\
 &= 6 \cdot 10^{38} \cdot 0.1 \cdot 7 \cdot 10^{-25} \cdot 0.01 \cdot 0.01 \cdot 0.2 \cdot 6 \cdot 10^{14} \cdot 0.25 \\
 &\approx 10^{-8} / \text{sec} \quad \approx 60 / \text{day} \quad (\text{at } 70\% \text{ overall efficiency})
 \end{aligned}$$

This scenario relies on the availability of two high resolution spectrometers with momenta around 2 GeV/c. It is compatible with the present plan for the CEBAF experimental equipment which sees initially a 4 GeV/c and a 3 GeV/c spectrometer.

b) Accidental coincidence rate for θ_e and θ_K around 15°

For the calculation of the accidental coincidences the single counting rate in both spectrometers has to be known. To determine the signal-to-noise (S/N) ratio the noise was integrated in a 1 MeV bin (corresponding to twice the FWHM missing mass resolution, see section c). The inelastic electron scattering cross section per nucleon has been estimated from a DESY measurement /10/ to be

$$d^2\sigma/d\Omega_e \cdot dE_e = 0.2 \mu\text{barn}/\text{sr} \cdot \text{GeV}$$

In a one MeV bin this leads to an electron rate

$$\begin{aligned} N_e &= (L/A) \rho d A d^2\sigma/d\Omega_e \cdot dE_e \cdot \Delta\Omega_e \cdot \Delta E_e \cdot N_e \\ &= 6 \cdot 10^{23} \cdot .1 \cdot 2 \cdot 10^{-31} \cdot .01 \cdot .001 \cdot 6 \cdot 10^{14} = 70/\text{sec} \end{aligned}$$

The total K^+ production rate is difficult to estimate because virtual photons in the wide energy range between $E_\gamma - E_e$ and E_e can contribute. In addition to the $\gamma p \rightarrow K^+ \Lambda$ process, Σ production, the excitation of the higher Λ and Σ states, the photoproduction of K^* and even the coherent nuclear production of the ϕ ($\phi \rightarrow K^+ K^-$) have to be taken into account. Without using detailed models for these reactions, one can assume that, at high energies, $\sigma_{\text{tot}}(\gamma p \rightarrow K^+ X)$ is 4 μb per nucleon. With additional assumptions on the angular dependence of the inclusive cross section and on the K^+ momentum spectrum, one obtains an estimate for the double differential cross section at forward angles in the laboratory system

$$d^2\sigma/d\Omega_K \cdot dp_K \approx 5 \cdot 10^{-33} / \text{sr} \cdot \text{MeV}/c \quad \text{per nucleon}$$

The flux of virtual photons in the forward direction is approximately described /9/ by

$$dN_\gamma = a' N_e (dE_\gamma/E_\gamma) \quad \text{with } a' \approx .02$$

The integration over the active photon energy range yields

$$N_{\gamma} = \alpha' \cdot N_e \cdot \ln(E_o / (E_o - E_e))$$

$$= .02 \cdot 6 \cdot 10^{14} \cdot \ln 2 = 8.3 \cdot 10^{12} / \text{sec}$$

leading to a kaon rate in a one MeV bin

$$N_K = (L/A) \cdot \rho d \cdot A \cdot d^2\sigma/d\Omega_K \cdot dp_K \cdot \Delta\Omega_K \cdot \Delta p_K \cdot N_{\gamma} \cdot \epsilon_K$$

$$= 6 \cdot 10^{23} \cdot .1 \cdot 5 \cdot 10^{-33} \cdot .01 \cdot 1 \cdot 8.3 \cdot 10^{12} \cdot .25$$

$$\approx 6 / \text{sec}$$

Now the accidental rate can be calculated: $N_{acc} = N_e \cdot N_K \cdot \tau \cdot d$.

Using a coincidence resolving time of $\tau = 2$ nsec (corresponding to the bunch separation in one of the three CEBAF beams) and a duty-cycle $d=1$ one obtains

$$N_{acc} = 70 \cdot 12 \cdot 2 \cdot 10^{-9} \cdot 1 = 1.7 \cdot 10^{-6} / \text{sec}$$

Since the real rate in a one MeV bin is $5 \cdot 10^{-6} / \text{sec}$, the resulting S/N ratio is approximately 6. Note that this value depends critically on the assumptions for inclusive kaon production.

The total hadronic production rate in the target is estimated to be of the order of 10^9 particles/sec, making the observation of coincident hadrons from the hypernuclear decays in a large acceptance detector impossible. The rate of true charged particles within the momentum acceptance of the kaon spectrometer approaches 1 Mc/s which will make kaon identification (especially on-line) a difficult task.

c) Missing mass resolution for θ_e and θ_K around 15°

To estimate the excitation energy resolution for the hypernucleus, it has been assumed that the momentum spread of the initial electron and the momentum resolution of the outgoing e' and the kaon is 10^{-4} . To simplify the calculation, the approximation

$$dM_x \approx dE_o + dE_e + dp_K + (E_\gamma \cdot p_K \cdot \theta_K / M_x) \cdot d\theta_K$$

has been used. This leads to the following contributions to the total missing mass resolution

primary beam	$(10^{-4}$ of 4 GeV/c)	400 keV
outgoing electron	$(10^{-4}$ of 2 GeV/c)	200 keV
outgoing kaon	$(10^{-4}$ of 1.8 GeV/c)	180 keV
kaon energy loss and straggling		200 keV

total		520 keV

The main contribution comes from the 10^{-4} energy spread of the incident electron beam. In the superconducting CEBAF accelerator, the spread is mainly caused by

- (1) the length of the bunches and the corresponding cosine variation of the RF voltage
- (2) the long term variation of the RF voltage

To go well beyond an missing mass resolution of 500 keV will not only require a substantial improvement of the incident beam (like using a dispersed beam at the target in combination with either dispersion matching or re-imaging techniques) but also the use of a thinner target. This will further reduce the (already small) coincidence counting rate. Compensating for the lower target thickness by using higher incident currents is practically impossible because of beam power limitations.

2. $(e,e'K^+)$, $\theta_e \approx 0^\circ$

Following a suggestion by C.E. Hyde-Wright et al. /9/, this set-up makes use of the high flux of quasi-real photons produced by electrons scattered at small angles. Since there is no longer a need to boost the Mott cross section by going to high electron energies, the primary energy can be relatively low which will make the task of getting high absolute energy resolution easier.

A possible arrangement for using 0° electron scattering is shown in fig. 5. The photon energy is tagged by the detection of the corresponding electron in a broad-band, but small solid angle, magnetic spectrometer. A split pole design /15/ is especially suitable to cover the required momentum range of (.1-.35) GeV/c simultaneously. Kaons are detected in a high resolution spectrometer with a moderate maximum momentum (like e.g. the 1.2 GeV/c spectrometer designed by R. Neuhausen /12/). Outgoing electrons and kaons have to be separated using a common transverse magnetic field. It may be possible to utilize the first magnet of the split pole for this task. It has to be investigated how this will affect the optical properties of the kaon spectrometer.

The 0° set-up is not directly compatible with the present design of the high resolution spectrometers. A short, large solid angle spectrometer would be ideal for K^+ detection. The present 3 GeV/c spectrometer is remarkably short, making it possible to use it for kaons with momenta well below 3 GeV/c. Its solid angle, however, is about a factor of 3 smaller than what has been assumed for the previous counting rate calculations. In addition, a broad band, but low energy, electron spectrometer would be needed. (Several split-pole spectrometers have been built; there may be one available on loan.)

a) True coincidence rate for $\theta_e \approx 0^\circ$

The coincidence rate was calculated under the following assumptions

initial e^- energy	$E_e = 1.7 \text{ GeV}$	
incident flux	$N_e = 2 \cdot 10^{12} / \text{sec}$	(I=300nA)
target thickness	$\rho \cdot d = 10 \text{ mg/cm}^2$	(^{12}C)
luminosity	$L = 1.2 \cdot 10^{34} \text{ cm}^{-2} \cdot \text{sec}^{-1}$	per nucleon
final e^- energy	$E_e = (.1-.35) \text{ GeV}$	
K^+ solid angle	$\Delta\Omega_K = 35 \text{ msr}$	

$$N_{eK} = L/A \cdot \rho d \cdot d\sigma/d\Omega_K \cdot \Delta\Omega_K \cdot N_\gamma \cdot \epsilon_K$$

(Note that only the product of target thickness and beam intensity enters the rate calculation. A 10 mg/cm^2 target gives a negligible contribution to the overall resolution). Using a cross section of 55 nb/sr (averaged over the acceptance of the kaon spectrometer) and $N_\gamma \approx .015 \cdot N_e \cdot dE_\gamma/E_\gamma$ yields about the same count rate as the high luminosity set-up:

$$N_{eK} = (6 \cdot 10^{23} / 12) \cdot .01 \cdot 55 \cdot 10^{-33} \cdot .035 \cdot .015 \cdot 3 \cdot 10^{12} \cdot (.25/1.5) \cdot .25$$

$$\approx 1.2 \cdot 10^{-8} / \text{sec} \quad (\approx 70 / \text{day} \text{ at } 70\% \text{ overall efficiency})$$

b) Accidental coincidence rate for $\theta_e \approx 0^\circ$

The electron rate is totally dominated by bremsstrahlung production; it can be approximately described by

$$dN_e = (X/X_0) \cdot (dE_e/E_\gamma) \cdot N_e$$

where X/X_0 is the target thickness in units of radiation lengths and E_γ is the energy of the quasi-real photon: $E_\gamma = E_e - E_e'$. The electron rate in a 1 MeV bin is

$$\Delta N_e \approx (.01/42.7) \cdot (.001/1.5) \cdot 2 \cdot 10^{12} \approx 3 \cdot 10^5 / \text{sec}$$

As in the case of a bremsstrahlung tagging system, two different types of accidental coincidences have to be distinguished

- (i) Two electron counters fire simultaneously (one real and one accidental hit). Events of this type will be rejected if both electron hits (combined with the kaon information) lead to hypernuclear excitation energies within the small region of interest. Therefore, there will be no contribution to the accidental coincidence rate. A small correction will have to be applied to the cross sections to account for the loss of events.
- (ii) The kaon has been produced by photons above the photon energy range covered by the electron spectrometer. One electron counter gave a random signal leading to an accidental coincidence that will be accepted as a true event. The accidental contribution can be subtracted by measuring delayed coincidences. The total K^+ production rate is easy to estimate because only the $K^+\Lambda$ final state can contribute.

$$d\sigma/d\Omega_K \approx 1.6 \mu\text{b/sr} \text{ per proton (in the lab. system)}$$

The virtual photon rate per MeV is

$$\begin{aligned} dN_\gamma &\approx \alpha' \cdot N_e \cdot dE_\gamma/E_\gamma \\ &\approx .015 \cdot 2 \cdot 10^{12} \cdot .001/1.65 \approx 1.8 \cdot 10^7 / \text{sec} \end{aligned}$$

The kaon rate in a one MeV bin is

$$\begin{aligned} dN_K &= L/A \cdot \rho d \cdot (A/2) \cdot d\sigma/d\Omega_K \cdot \Delta\Omega_K \cdot dN_\gamma \cdot \epsilon_K \\ &= 3 \cdot 10^{23} \cdot .01 \cdot 1.6 \cdot 10^{-28} \cdot .035 \cdot 1.8 \cdot 10^7 \cdot .25 \\ &= 7.5 \cdot 10^{-4} / \text{sec} \end{aligned}$$

Now the accidental rate can be calculated

$$\begin{aligned}
 N_{\text{acc}} &= N_e \cdot N_K \cdot \tau \cdot d \\
 &= 3 \cdot 10^5 \cdot 7.5 \cdot 10^{-4} \cdot 2 \cdot 10^{-9} \cdot 1 = 4.5 \cdot 10^{-7} / \text{sec}
 \end{aligned}$$

Since the real rate per level is $\approx 4.8 \cdot 10^{-6} / \text{sec}$ the S/N ratio for 0.5 MeV bins is ≈ 20 , larger than for the high luminosity set-up.

The total hadronic production rate in the target is of the order of $2 \cdot 10^5$ particles/sec (nearly 4 orders of magnitude lower than for the high intensity set-up). Therefore, detection of coincident particles from the decay of the hypernucleus in a simple large acceptance detector should be possible.

c) Missing mass resolution for $\theta_e \approx 0^\circ$

Again, it has been assumed that the momentum spread for the initial electron and the final kaon is 10^{-4} . The momentum resolution for the outgoing electron was taken to be $2 \cdot 10^{-4}$ because of the wide momentum band that has to be covered. This leads to the following contributions to the total missing mass resolution

primary beam	(10^{-4} of 1.7 GeV/c)	170 keV
outgoing electron	($2 \cdot 10^{-4}$ of 0.25 GeV/c)	50 keV
outgoing kaon	(10^{-4} of 1.2 GeV/c)	120 keV
kaon energy loss and straggling		30 keV
uncertainty caused by 2 mrad angular resolution		30 keV
total		<hr/> 220 keV

In contrast to the high intensity set-up, there is still considerable room for improvements:

- (1) because only a low intensity beam is required, there are several possibilities to reduce the momentum spread of the incident electron beam. At the accelerator level, the lower micro-bunch loading may

lead to a reduced bunch width. Independent of improvements to the accelerator, a high dispersion beam transfer line between the accelerator and the experimental area and a target with a small transverse extension (e.g. a thin wire) will reduce the momentum spread of the fraction of the beam hitting the target. A high dispersion beam line would also be very useful to determine and improve the momentum stability of the accelerator.

- (2) the spectrometer for the outgoing electrons is not pushing the state-of-the art ($2 \cdot 10^{-4}$ resolution has been reached in broad band spectrometers, like the Enge split-pole, without using soft-ware corrections)
- (3) the design for the QQDD 1.2 GeV spectrometer /12/ features a dispersion/magnification ratio of 15.4 meters and an angular resolution of ≤ 1 mrad. This is an excellent basis for aiming at a resolution of the order of several 10^{-5} (a very small beam spot on the target and substantial soft-ware corrections to account for higher order aberrations will be essential).
- (4) the kaon energy loss and straggling can be further reduced by using a thinner target. The resulting loss in counting rate may be compensated by increasing the beam current; counting rates and S/N ratio will stay the same. A very clean beam will be required because of the increased sensitivity of the set-up to beam associated background (beam halo, backscattering from the beam dump).

These improvements rely heavily on the availability of an electron beam with unprecedented quality. The final resolution is difficult to predict. There is, however, reason to believe that a missing mass resolution of the order of 100 keV can be achieved.

3. Comparison of the two methods

The basic operating conditions for the two methods are summarized in Table I. The main advantage of the high luminosity set-up is that standard laboratory equipment can be used for the (e,e'K) program. The main disadvantage is that the high luminosity makes the detection of coincident hadrons (which will have little or no angular correlation with the outgoing kaon) impossible.

Coincident detection of hadrons from the hypernuclear decay can provide useful additional information on hypernuclei, in particular:

- (a) distinguish between the different decay modes of the hypernucleus. Except for light hypernuclei, the $\Lambda \rightarrow N\pi$ decay is strongly Pauli suppressed. Therefore, the strangeness changing $\Lambda N \rightarrow NN$ interaction becomes the dominant decay mode. The ratio $(\Lambda \rightarrow N\pi)/(\Lambda N \rightarrow NN)$ will give information on the strength and the density dependence of the $\Lambda N \rightarrow NN$ interaction.
- (b) determine the lifetime of hypernuclei. There are competing mechanisms influencing the hypernuclear lifetime τ . Pauli suppression of the Λ decay will increase τ , whereas the open $\Lambda N \rightarrow NN$ channel will decrease it. The present information on the lifetime of hypernuclei is very scarce /16,17/. Typical values for τ are 100 psec, about half the lifetime of the free Λ . The lifetime can be determined by
 - (1) measuring directly the time delay distribution between the K^+ emission and the the emission of the decay products. This is difficult because the lifetime is much smaller than the time resolution presently achievable.
 - (2) measuring the path length distribution of the hypernucleus between production and decay as sketched in fig. 6. A light

hypernucleus like ${}^{12}\text{B}_\Lambda$ will travel on the average about 1 mm before it decays. Since the velocity of the hypernucleus can be accurately calculated from the scattered electron and the kaon, the path length distribution can be converted directly into a time distribution. Very thin targets (of the order of $100 \mu\text{g}/\text{cm}^2$), an intense narrow electron beam ($100 \mu\text{A}$ current, width about $100 \mu\text{m}$) and a precision vertex detector (e.g. using solid state microstrips) will be essential for this challenging experiment. It can only be performed at low luminosity.

(c) improve the signal-to-noise ratio by

- (1) using the detection of quasifree Λ as a veto. If Λ production does not lead to the formation of a hypernucleus, the Λ has to escape (possibly after quasifree ΛN scattering). It will typically travel about 2 cm before it decays into πN . At least the $p\pi^-$ mode should be easy to detect.
- (2) using the detection of a decay vertex slightly outside of the target as a tagging signal for hypernuclear production. This would essentially suppress all other reactions (at a luminosity of $10^{34} \text{cm}^{-2}\text{sec}^{-1}$, the total production rate of stable hypernuclei is of the order of 1/sec). In view of the modest signal-to-noise ratio that can be obtained from electron-kaon coincidences alone, this method would be very valuable for the detection of weakly excited states.
- (3) enhance the signal for Σ hypernuclei. There is (somewhat controversial) evidence for the formation of Σ -hypernuclei from (K,π) reactions. The main problem is that Σ -hypernuclei form broad structures on top of quasifree Λ production. Detection of hadrons that can only be emitted after Σ -production has been crucial to enhance these structures /13/.

The main technical difficulty of the 0° (e,e'K) set-up is the high rate of electrons from the bremsstrahlung process in the forward tagging spectrometer. For the ^{12}C example, the rate in the focal plane detector per second is $\approx 4 \cdot 10^4/\text{mm}$ with a resolution requirement of $\approx 300 \mu\text{m}$. For a given amount of target material, the electron rate increases with the thickness in radiation length. Due to the rising accidental contribution, this will make the investigation of heavy hypernuclei difficult unless schemes to enhance the signal for hypernuclear production can be used.

E. Summary and Conclusions

The basic features of the electromagnetic excitation of hypernuclei have been discussed. Two experimental scenarios have been found to be suitable for the investigation of this reaction at CEBAF. The standard (e,e'K) solution relies on the pair of high resolution spectrometers planned for Hall A. Greater flexibility for detecting coincident hadrons and higher resolution for the excitation energy of the hypernucleus seem to be achievable by using forward scattered electrons to produce a high flux of quasi-real tagged photons. However, this solution requires experimental equipment which will presumably not be available for the first round of experiments.

Taking the limited resources of the laboratory into account, and also in view of the theoretical uncertainties, it seems to be wise to start the hypernuclear program at CEBAF using the standard spectrometer set-up. The decision to build a specialized set-up would then be based on the results of the first experiments.

For both methods, an incident electron beam of unprecedented quality (as it will be available from the superconducting CEBAF accelerator) is absolutely essential for the success of the experiment.

F. References

- /1/ see e.g. the talks by B. Bassalleck, L.S. Kisslinger and R.A. Eisenstein, Proc. of the Steamboat Springs Meeting, 1984, AIP Conf. #123
- /2/ T. Walcher, Nucl. Phys. A434 (1985) 343c
- /3/ T.W. Donnelly, Lecture Notes in Physics 234 (1984) 309
- /4/ A.M. Bernstein, Proc. of the Conference on Hypernuclear and Kaon Physics, Heidelberg 1982, MPIH-1982-V20
- /5/ S.S. Hsiao and S.R. Cotanch, Phys. Rev. C28 (1983) 1668
- /6/ J. Cohen, Phys. Lett. 153B (1985) 367
- /7/ J. Cohen, Contribution to the CEBAF 1986 Summer Study Report (RPAC II)
- /8/ C. Bennhold and L.E. Wright, Proc. of the Lake Louise Meeting, 1986, AIP Conf. #150, p. 914
- /9/ T.W. Donnelly, Proc. of the 1985 CEBAF Summer Workshop
- /10/ G. Mecklenbrauck, DESY internal report F23-80/02 (1980)
- /11/ C.E. Hyde-Wright et al., MIT-LNS preprint DOE/ER 03069-357A (1985) and Proc. of the 1985 CEBAF Summer Workshop
- /12/ R. Neuhausen, Proc. of the 1986 CEBAF Summer Study (RPAC I) 11-31
- /13/ J. Chiba, Proc. of the Lake Louise Meeting, 1986, AIP Conf. #150, p. 917
- /14/ J. Mougey, Proc. of the 1986 CEBAF Summer Workshop and CEBAF Spectrometer Notes
- /15/ J.E. Spencer and H.A. Enge, Nucl. Instr. Meth. 49 (1967) 181
- /16/ J. Dubach, Int. Symposium on Weak and Electromagnetic Interactions in Nuclei, Heidelberg 1986
- /17/ R. Grace et al., Phys. Rev. Lett. 55 (1985) 1055

Figure Captions

Figure 1: Differential cross section for the elementary reaction
 $\gamma p \rightarrow K^+ \Lambda$

Figure 2: Momentum transfer q to the final hypernucleus as a function of the kaon laboratory angle in the reaction
 $\gamma {}^{12}\text{C} \rightarrow K^+ {}^{12}\text{B}_\Lambda$

Figure 3: Differential cross section for the reaction $\gamma {}^{12}\text{C} \rightarrow K^+ {}^{12}\text{B}_\Lambda 1^- : (1s1/2) (1p3/2)^{-1}$ as a function of the kaon laboratory angle. The curves are the result of the parametrization described in the text.

Figure 4: Average differential cross section for the reaction $\gamma {}^{12}\text{C} \rightarrow K^+ {}^{12}\text{B}_\Lambda 1^- : (1s1/2) (1p3/2)^{-1}$ as a function of the incident photon energy. The averaging was performed in the kaon angular range between 1° and 6° .

Figure 5: Experimental set-up for the study of hypernuclear production using 0° electron scattering.

Figure 6: Schematic set-up for the lifetime determination via the decay length measurement. T target, DV decay vertex, VD1 and VD2 vertex detectors to track the hadrons h_1 and h_2 .

Table I: Comparison of the high and low luminosity set-ups

	high luminosity	low luminosity
Luminosity [$\text{cm}^{-2}\text{sec}^{-1}\text{nucleon}^{-1}$]	$3.6 \cdot 10^{37}$	$1.2 \cdot 10^{34}$
incident energy [GeV]	4.0	1.7
e' energy [GeV]	2.0	0.1-0.35
e' solid angle [msr]	10	1
scattered e^- /sec/Mev/c	70	$3 \cdot 10^5$
K^+ mean momentum [MeV/c]	1.8	1.2
K^+ solid angle [msr]	10	35
K^+ /sec/Mev/c	6	$7.5 \cdot 10^{-4}$
real coincidence rate [sec^{-1}]	10^{-8}	10^{-8}
signal-to-noise	6	20
hadronic rate in 4π [sec^{-1}]	10^9	$2 \cdot 10^5$
hadron rate within the acceptance of the kaon spectrometer /sec	10^6	50
e^+ rate within the acceptance of the kaon spectrometer /sec	??	$6 \cdot 10^5$ *)

*) This value corresponds to a worst-case scenario with the kaon spectrometer covering 0° without any mechanical obstruction of the central part of the acceptance.

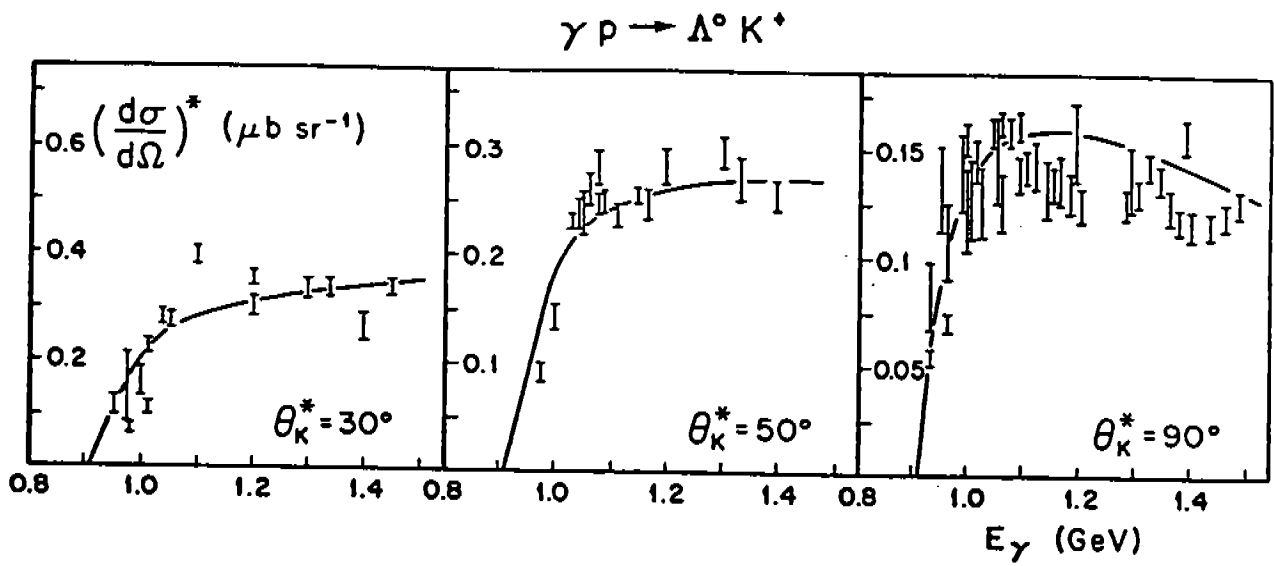


Figure 1: Differential cross section for $\gamma p \rightarrow K^+ \Lambda$

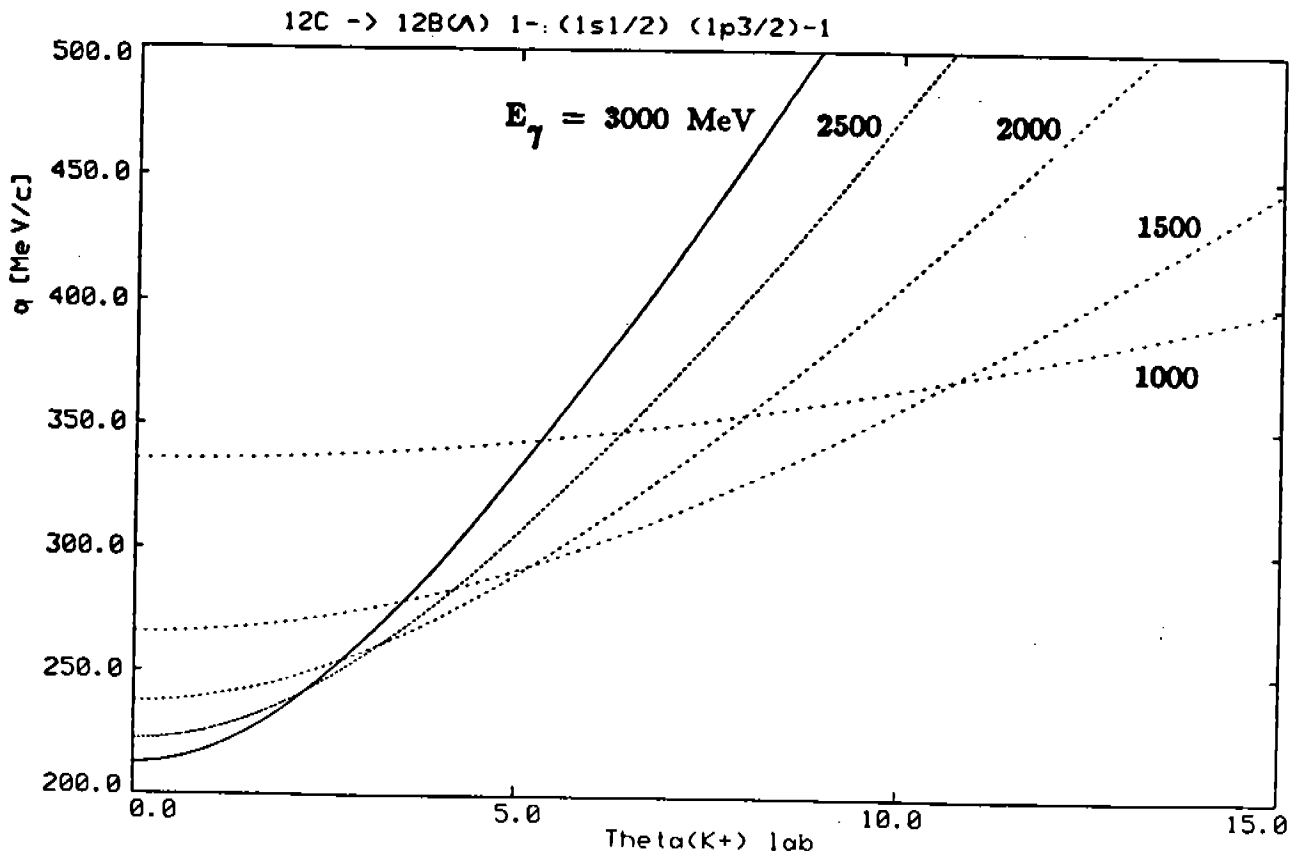


Figure 2: Momentum transfer q as a function of θ_K for $\gamma ^{12}\text{C} + K^+ ^{12}\text{B}_\Lambda$

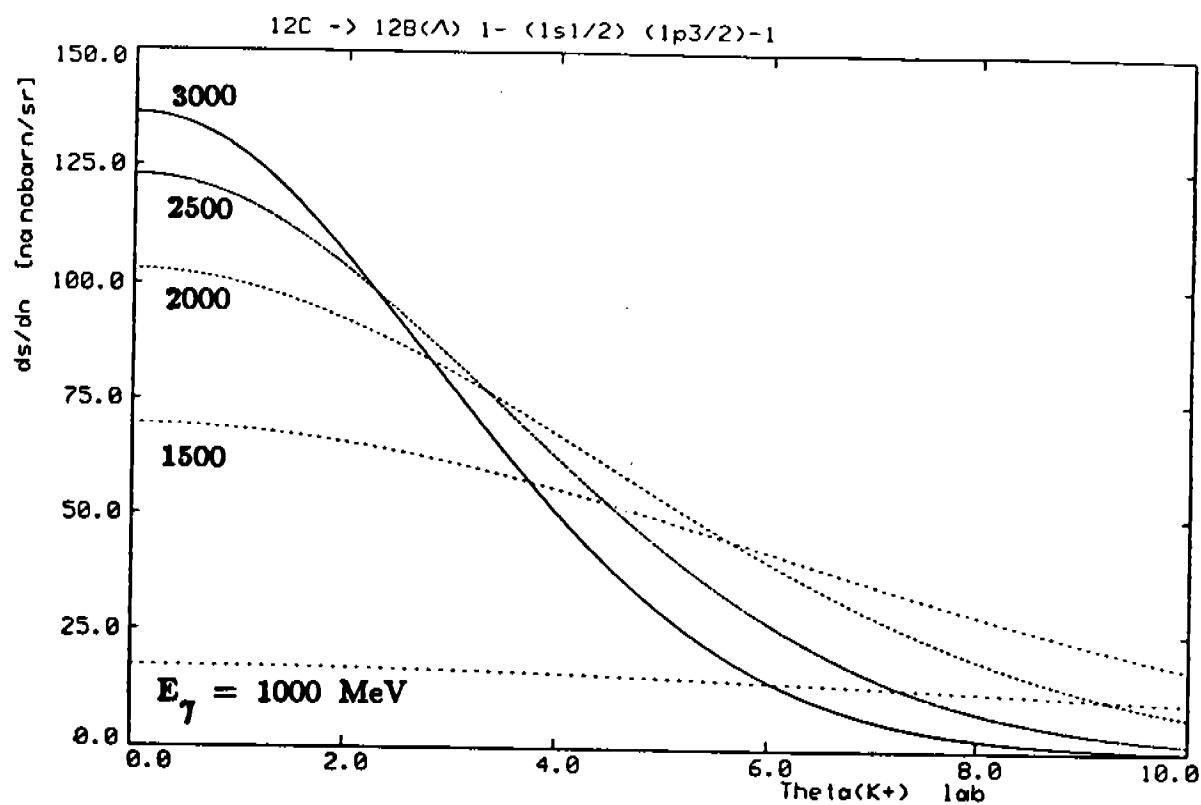


Figure 3: $d\sigma/d\Omega_{\mathbf{K}}$ for γ $^{12}\text{C} + \text{K}^+ \rightarrow ^{12}\text{B}_{\Lambda} 1^- : (1s1/2) (1p3/2)^{-1}$ as a function of $\theta_{\mathbf{K}}$

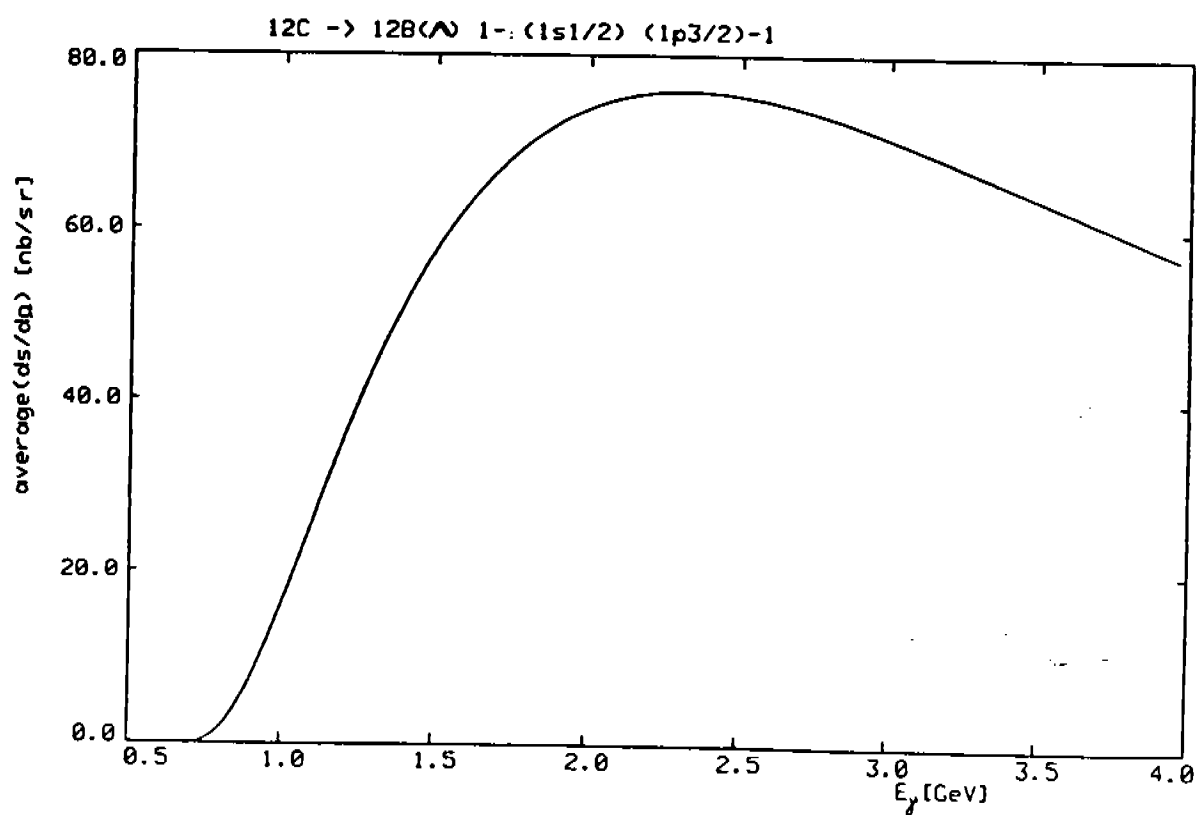


Figure 4: Average $d\sigma/d\Omega_{\mathbf{K}}$ for γ $^{12}\text{C} + \text{K}^+ \rightarrow ^{12}\text{B}_{\Lambda} 1^- : (1s1/2) (1p3/2)^{-1}$

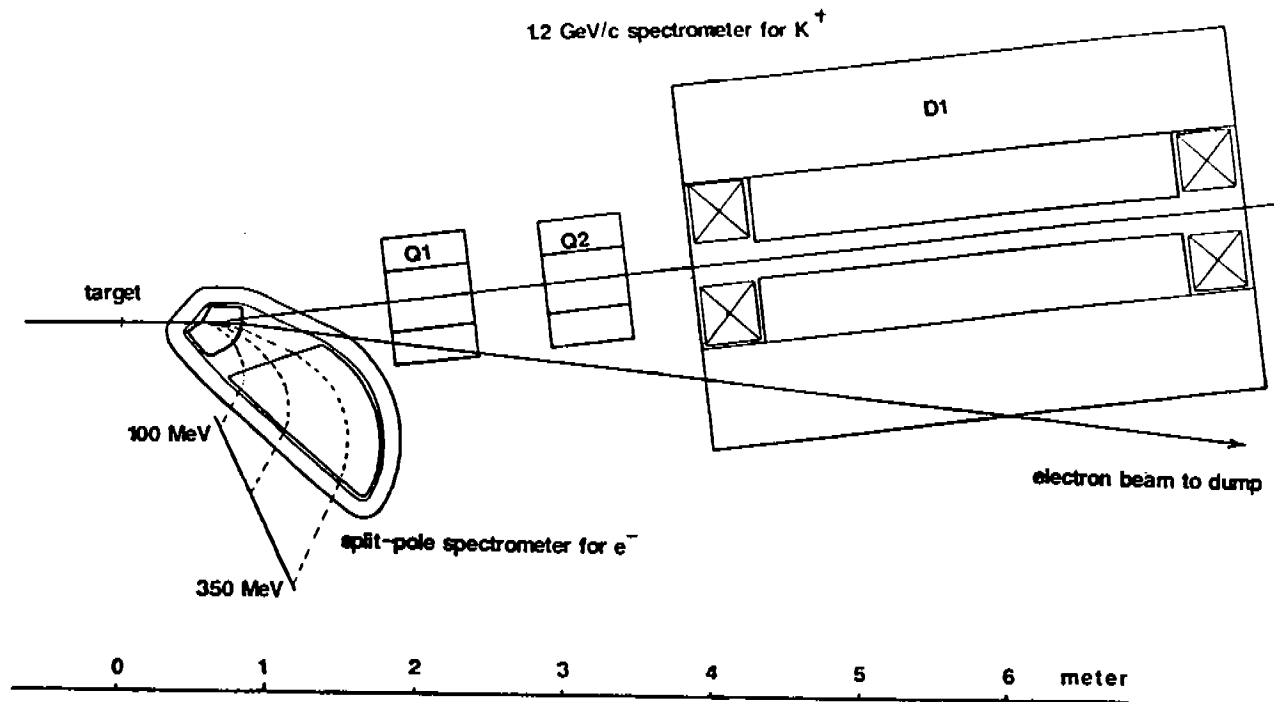


Figure 5: 0° electron scattering set-up

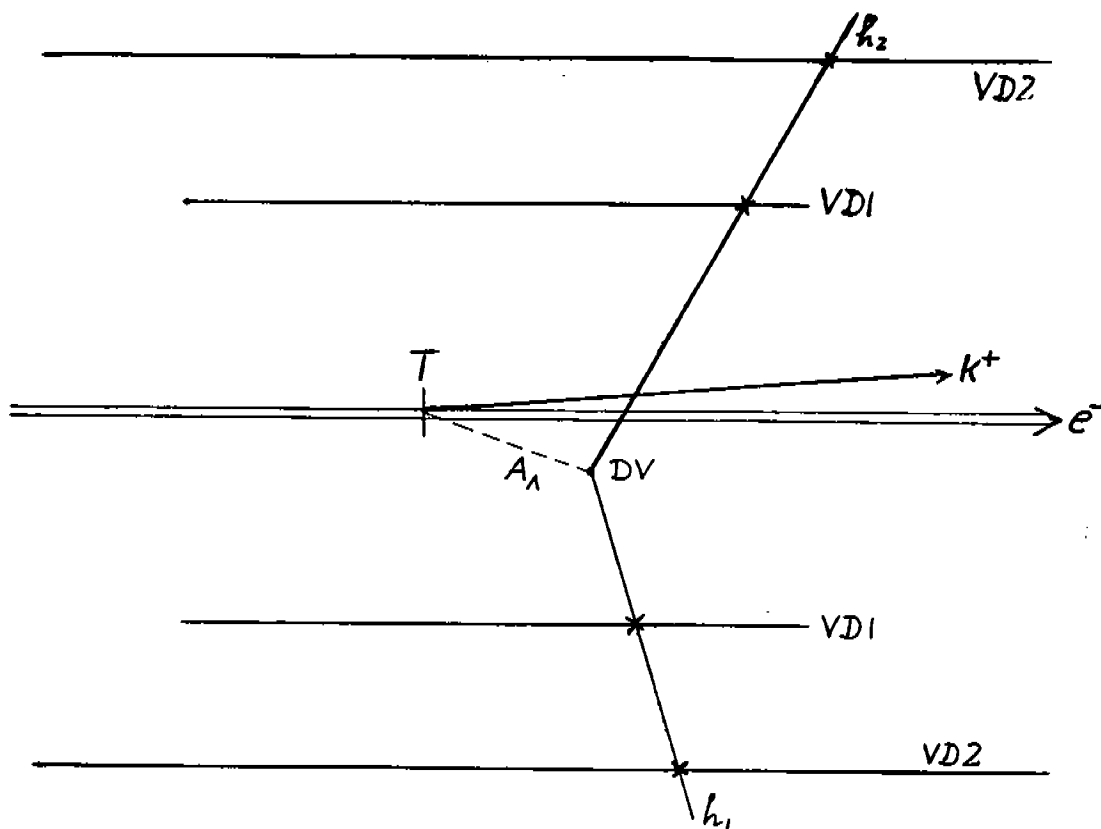


Figure 6: Schematic set-up for the decay length measurement